ACS APPLIED MATERIALS & INTERFACES

Research Article

www.acsami.org

Interfacial Engineering of Carbon Nanofiber–Graphene–Carbon Nanofiber Heterojunctions in Flexible Lightweight Electromagnetic Shielding Networks

Wei-Li Song,[†] Jia Wang,[†] Li-Zhen Fan,*[,†] Yong Li,[‡] Chan-Yuan Wang,[§] and Mao-Sheng Cao*[,‡]

[†]Institute of Advanced Materials and Technology, University of Science and Technology Beijing, Beijing, 100083, P. R. China

[‡]School of Materials Science and Engineering, Beijing Institute of Technology, Beijing, 100081, P. R. China

[§]310 Department, Third Institution of China Aerospace Science & Industry, Beijing 100071, P. R. China

Supporting Information

ABSTRACT: Lightweight carbon materials of effective electromagnetic interference (EMI) shielding have attracted increasing interest because of rapid development of smart communication devices. To meet the requirement in portable electronic devices, flexible shielding materials with ultrathin characteristic have been pursued for this purpose. In this work, we demonstrated a facile strategy for scalable fabrication of flexible all-carbon networks, where the insulting polymeric frames and interfaces have been well eliminated. Microscopically, a novel carbon nanofiber–graphene nanosheet–carbon nanofiber (CNF–GN–CNF) heterojunction, which plays the dominant role as the interfacial modifier, has been observed in the as-fabricated networks. With the presence of CNF–GN–CNF heterojunctions, the all-carbon networks exhibit much increased electrical properties, resulting in the great enhancement of EMI shielding performance. The related mechanism for engineering the CNF interfaces based on the CNF–GN–CNF heterojunctions has been discussed. Implication of the results suggests that the lightweight all-carbon networks, whose thickness and density are much smaller than other graphene/polymer composites, present more promising potential as thin shielding materials in flexible portable electronics.

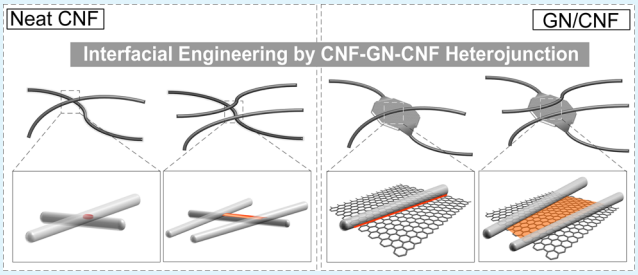

KEYWORDS: *flexible, graphene, heterojunctions, interfacial engineering, electromagnetic shielding*

INTRODUCTION

Flexible electronic devices have attracted increasing attention due to various advantages such as being lightweight, having small thickness, and having easy portability and promised broad applications in the electronic industry. Electromagnetic irradiation, generated in the operating electronics and circuits, has been considered as a significant concern due to the impact in the communication systems.[1−4] Therefore, novel lightweight carbon-based materials with excellent flexibility and high-performance electromagnetic interference (EMI) shielding have been largely pursued since those seem to be the most promising substitutes for traditional metal materials.[1−8]

In the early progress, foam composites embedded with carbon fibers (CFs) and carbon nanotubes (CNTs) were developed by Gupta's groups, demonstrating a novel approach for achieving lightweight shielding materials.[1,2] On the basis of this concept, researchers have employed other carbon fillers into the polymeric matrices to fabricate foam composites for EMI shielding.[9−14] According to a recent report of graphene materials, low electrical conductivity in the graphene-based foam structures may result in insufficient shielding performance (less than 20 dB), which is primarily due to the inadequate conductive networks established in these porous structures.[9,15] For targeted EMI shielding applications (commercial application shielding level > 20 dB), different strategies have also been largely explored more recently.[14,16] In a typical study, graphene/poly(dimethylsiloxane) (PDMS) composite foams were developed based on chemical vapor deposition (CVD) of graphene onto Ni-foam frameworks. The resultant structures exhibited improved conductive connection (~200 S/m) with a shielding effectiveness of 22–25 dB (~1 mm in foam thickness) over the frequency range of 8.2–12.4 GHz (X band).[14] Very recently, flexible graphene/poly(ethylene/vinyl acetate) (PEVA) composite films with electrical conductivity ≈ 250 S/m have presented a similar shielding performance (23–27 dB) but with a large decrease in the thickness of the composite films (~0.36 mm).[16]

Additionally, other exploratory studies have demonstrated that use of carbon-based hybrid configurations could be an effective approach in the improvement of conductive paths.[17−21] In a recent work, multiwalled carbon nanotubes (MWCNTs) were mechanically mixed with polystyrene (PS)/graphite nanoplate (GNP) beads, followed by being processed into PS/MWCNT/GNP composites. In the presence of

Received: April 7, 2014
Accepted: June 9, 2014
Published: June 10, 2014

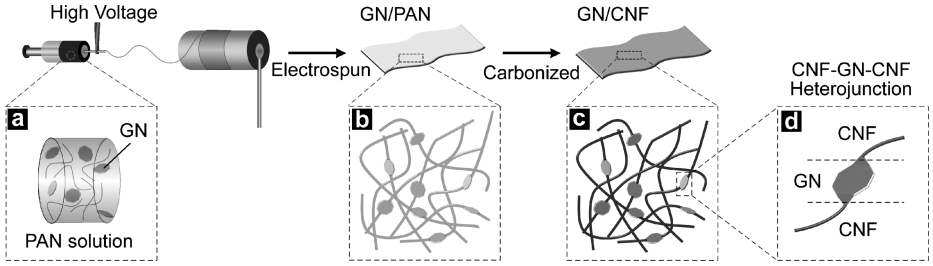

Figure 1. Scheme for fabricating flexible networks and CNF−GN−CNF heterojunctions. Typical schemes of the GN/PAN solution (a), polymer−GN heterojunctions (b), and CNF−GN−CNF heterojunctions (c and d).

MWCNTs, electrical conductivity was observed to be greatly improved in the resulting PS/MWCNT/GNP, and an effective shielding ≈ 20.2 dB was obtained.[17] Similarly, chemically reduced graphene oxides (rGOs) were found to effectively enhance the electrical conductivity and shielding performance of the CF/phenolic resin composites.[18] These studies indicate that the established conductive networks by mechanically mixing the multiphase carbon fillers are mostly responsible for the performance improvement.

According to previous work, it is noted that polymeric matrices mainly serve as robust frameworks in the flexible shielding composites, typically as the significant media for binding the mixed fillers.[9,10,12,13,15−18] Generally, a large filler amount is required in the insulating polymeric matrices in order to improve the electrical properties of the composites.[16,22,23] For materials of relatively poor electrical properties, however, more materials such as in thicker sheets or larger mass could be used to compensate for achieving the targeted EMI shielding results.[9,12,14] As a consequence, the flexibility and lightweight characteristic may be sacrificed. Here, in this work, we developed a flexible lightweight carbon composite which was formed by novel carbon nanofiber−graphene nanosheet−carbon nanofiber (CNF−GN−CNF) heterojunctions. In this configuration, the insulating polymeric matrix, polyacrylonitrile (PAN), was processed and converted into flexible conductive frames. With the presence of PAN, multilayer GN of high electrical conductivity was processed into CNF−GN−CNF heterojunctions, which serve as interfacial modifiers to enhance the electrical properties of the CNF networks. As expected, electrical conductivity of the GN/CNF composite networks has been largely increased due to introduction of the CNF−GN−CNF heterojunctions. Upon the interfacial engineering of the conductive networks with such configurations, the related mechanism for conductive enhancement has been discussed. Consequently, the flexible GN/CNF composite networks exhibited much enhanced EMI shielding performance (26−28 dB) at a small thickness (∼0.26 mm). These novel networks based on the CNF−GN−CNF heterojunctions promise great potential applications in the lightweight electronic devices.

RESULTS AND DISCUSSION

GN was prepared by direct exfoliation of expanded graphite in the acid environment, and the procedure was reported in our previous work.[24,25] In the as-prepared GN, most of the graphitic structures have been largely reserved in the exfoliation process and the oxygen concentration, associated with oxidized functional groups, was less than 10%.[25] These features indicate that the morphology and mass of the GN could be mostly preserved under high-temperature carbonization, and thus, the CNF−GN−CNF heterojunctions could be well retained. Furthermore, the electrical conductivity of the neat GN papers was measured to be ∼20 000 S/m,[25] suggesting great potential for increasing electrical properties of the CNF−GN−CNF heterojunctions.

The flexible GN/CNF composite networks were fabricated via the conventional electrospinning process (Figure 1). In the typical preparation, the liquid droplet of the viscous suspension (mixture of GN and PAN) was stretched under a high voltage and then a stream of liquid erupted, where the GN and polymer were connected via electrostatic interaction (mainly van der Waals forces). As the polymeric GN jet dried in flight, the connections were largely maintained in the form of polymer−GN heterojunctions (Figure 1b). The electrospun GN/polymer composite networks were stabilized at 270 °C in air and subsequently carbonized at 1000 °C in N_2. These treatments enabled the PAN fibers to be converted into CNFs (Figure 1c), by which the CNF−GN−CNF heterojunctions could be achieved (Figure 1d). Initial addition of GN in the polymer solution is shown in Table 1.

Table 1. Samples Used in This Work

	initial mass		carbonized networks		
	PAN (mg)	GN (mg)	CNF (mg)	GN (mg)	GN loading (wt %)
neat CNF	500		180		0
GN/CNF-1	500	20	180	18.7	9.4
GN/CNF-2	500	40	180	37.5	17.2
GN/CNF-3	500	90	180	84.3	31.9

The prepared free-standing GN/CNF composite networks were characterized by various techniques. Typical optical photos (Figure 2a) show a piece of GN/CNF composite networks, suggesting they are highly mechanically flexible and robust. According to the X-ray powder diffraction (XRD) patterns in Figure 2b, the broadened peak (located at ∼26°) in the GN sample indicates effective exfoliation of raw graphite.[24,25] As expected, the GN peak coupled with a broad carbonized CNF feature has been observed in the GN/CNF composite networks. Raman spectra exhibit the G band (∼1585 cm^{-1}) and D band (∼1350 cm^{-1}) of the measured samples (Figure 2c), demonstrating that the ratio of the D band to G band was decreased in the GN/CNF composite networks compared to that of neat CNF samples. As shown in Figure 2d, the results of thermogravimetric analysis (TGA) suggest that the residual masses of polymer and GN after 1000 °C carbonization under N_2 atmosphere were ∼36.1% and 93.5%, respectively. As listed in Table 1, the real GN masses and filler loadings in the GN/CNF composite networks were estimated based on the TGA results.

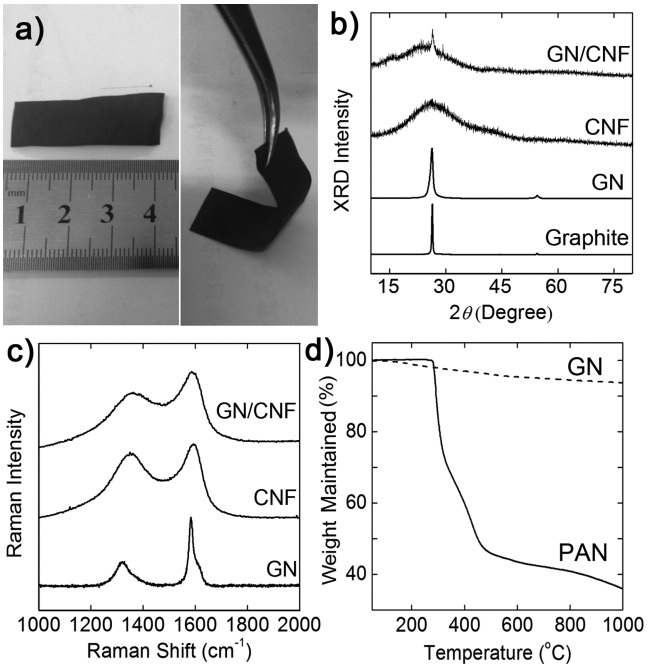

Figure 2. Photos of the flexible electrospun GN/CNF composite networks (a), XRD patterns (b), Raman spectra (c), and TGA analysis (d) of the samples as marked.

The morphologies of the as-prepared networks were achieved in scanning electron microscopy (SEM) and transmission electron microscopy (TEM). According to SEM images, Figure 3a shows a typical morphology of the as-prepared neat CNFs, suggesting uniform and continuous long fibers in the networks. The TEM image demonstrates that the neat CNFs are smooth with uniform diameters of 200−250 nm (Figure 3c and 3d). The SEM image of the GN/CNF composite networks (Figure 3b) exhibits that GN has been randomly embedded in the CNF networks. According to the TEM results, the GN used in this work presents a lateral size of several micrometers (Figure 4e) with a thickness of 4−6 nm

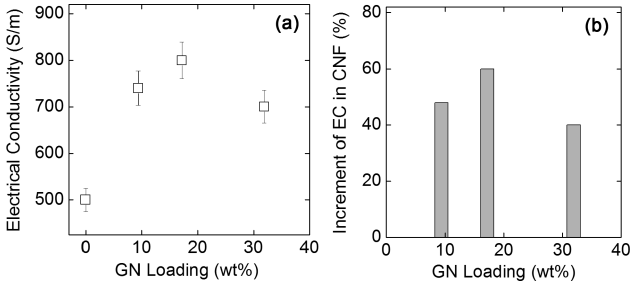

Figure 4. Electrical conductivity of the samples with different GN loadings (a). Increments of electrical conductivity (EC) in the GN/CNF composite networks based on the neat CNF networks (b).

(Figure 4f). Figure 4g exhibits a representative image of a CNF−GN−CNF heterojunction, suggesting that the CNFs were connected via GN bridging. The magnified image (Figure 4h) exhibits the tight connection of GN in the CNF−GN−CNF heterojunction.

The classical four-probe method was applied to measure the surface resistivity and electrical conductivity. After polymer was carbonized, the neat CNF networks presented conductive feature and corresponding electrical conductivity reached 500 S/m (Figure 4a). In the GN/CNF composite networks, the CNF−GN−CNF heterojunctions play a significant role in the enhancement of electrical conductivity. As shown in Figure 4b, electrical conductivity of the GN/CNF composite networks was found to approach 800 S/m. According to the electrical conductivity in the neat CNF networks, the increments of conductivity caused by different GN additions were calculated (Figure 4b).

In the GN/CNF composite networks with 9.4 and 17.2 wt % GN loadings, the pronounced enhancement in the electrical conductivity is mainly associated with the presence of GN. Specifically, it is suggested that formation of CNF−GN−CNF heterojunctions is responsible for modifying the interfaces of the CNF networks. In the composite networks, two major mechanisms were considered in the interfacial modification. First, CNF−GN−CNF heterojunctions could effectively reduce

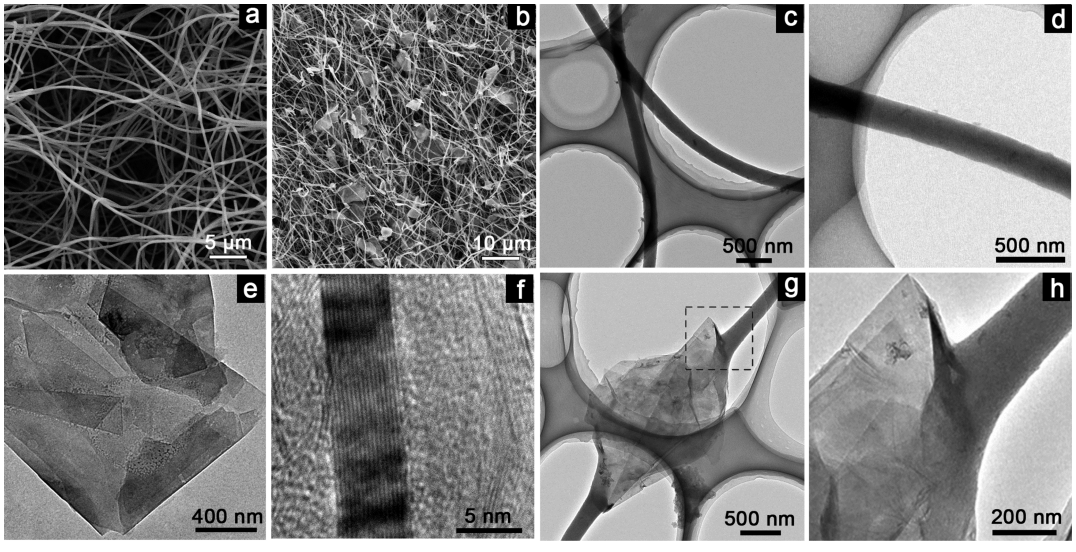

Figure 3. SEM images of the neat CNF networks (a) and GN/CNF composite networks (b); TEM images of the CNFs in neat CNF networks (c and d); TEM images of a piece of GN (e) and a cross-section view of the GN (f); typical TEM images of a CNF−GN−CNF heterojunction (g and h).

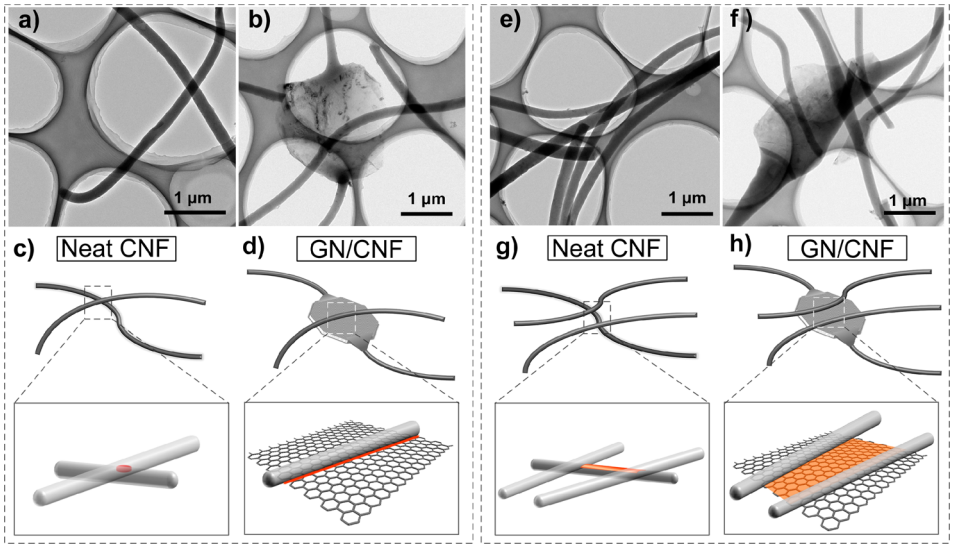

Figure 5. TEM image of two adjacent CNFs (a) and a scheme of related contact mode (c) in the neat CNF networks. TEM image of a cross formed by a CNF over a CNF−GN−CNF heterojunction (b), and a scheme of related contact mode (d) in the GN/CNF composite networks. TEM image of CNF bridges over adjacent CNFs (e), and a scheme of related bridging mode (g) in the neat CNF networks. TEM image of a bridge formed by a CNF−GN−CNF heterojunction (f), and a scheme of related bridging mode (h) in the GN/CNF composite networks. (The graphene motifs in the schemes are not to scale.)

the contact resistivity of adjacent CNFs. As demonstrated in the TEM image (Figure 5a), point contact is mainly considered as the contact mode between two adjacent fibers in the neat CNF networks (Figure 5c). However, in the presence of CNF−GN−CNF heterojunctions (Figure 5b), one-dimensional contact between CNFs and GN can be achieved (Figure 5d), which may increase the electrical conductivity of GN/CNF composite networks. On the other hand, the bridging mode in the CNF networks could be also modified by the CNF−GN−CNF heterojunctions. In the neat CNF networks, one-dimensional CNFs are the dominate bridges in the CNF networks (Figure 5c and 5g). In the GN/CNF composite networks, however, CNF−GN−CNF heterojunctions could serve as the bridges, and thereby conductive connections among CNFs could be improved by the two-dimensional conductive regions on the graphene surface (Figure 5f and 5h). Owing to these two major mechanisms for interfacial modification in the CNF networks, significant enhancement could be achievable in the electrical conductivity of the GN/CNF composite networks.

Interestingly, a slight decrease was found in the electrical conductivity (~700 S/m) of the GN/CNF composite networks with 31.9 wt % GN. Microstructures of the GN/CNF composite networks were analyzed based on the observation on the SEM (Figure 6). Nanoscopically, the fibers in the neat CNF networks present a smooth feature with a uniform diameter (Figure 6a and 6d). In the GN/CNF composite networks with 17.2 wt % GN, addition of GN at this level appears to have limited effects on the morphology and size of CNFs (Figure 6b), except for formation of CNF−GN−CNF heterojunctions (Figure 6e). Although 15−25% diameter shrinkage appears in the fibers after carbonization, no significant diameter change was observed in the fibers with the presence of 17.2 wt % GN, compared to the neat CNFs. According to the observation in the GN/CNF composite networks with 31.9 wt % GN, fractured nanofibers have been largely found in the networks, which could be understood in terms of the explanation that the increased amount of GN has

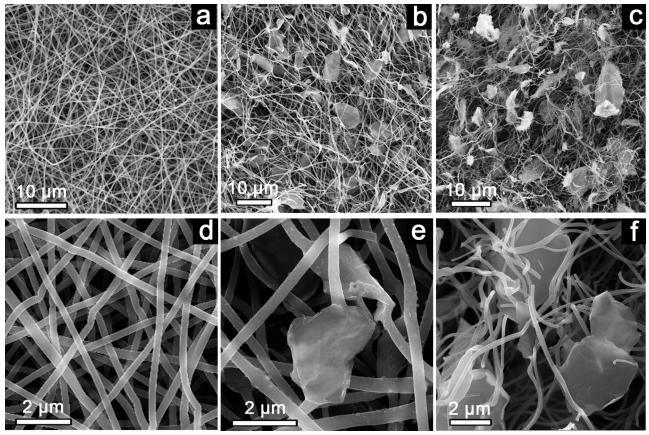

Figure 6. SEM images of neat CNF networks (a and d), GN/CNF composite networks with 17.2 wt % GN (b and e), and GN/CNF composite networks with 31.9 wt % GN (c and f).

A great impact on formation of robust continuous fibers. One of the factors may be associated with the rheological change due to the increased GN loading, and therefore, the flow rate was required to be changed in the electrospinning process.[26,27] As a consequence, CNFs of smaller diameters were observed in the GN/CNF composite networks with 31.9 wt % GN (Figure 6c and 6f), which leads to the diminishment in the mechanical properties and conductive connections of the fibers (Figure 6f). Hence, the electrospun GN/CNF composite networks with higher GN loading (31.9 wt %) were relatively mechanically brittle with A somewhat decrease in the electrical conductivity. The results of THE electrical properties and microscopic morphologies indicate that the GN/CNF composite networks with relatively lower GN additions should be ideal for scalable production of robust flexible networks.

To evaluate EMI shielding performance, the mechanically robust networks (neat CNF and GN/CNF composite networks with 9.4 and 17.2 wt % GN) were fabricated into sandwich layered structures[16,25] for measuring electromagnetic parame-

ters. Accordingly, the shielding effectiveness (SE) along with SE absorption and SE reflection was determined based on the measured *S* parameters (see Experimental Section). Due to the limited difference in the electrical conductivity, the GN/CNF composite networks with both 9.4 (Figure S1, Supporting Information) and 17.2 wt % GN (Figure 7) have very similar

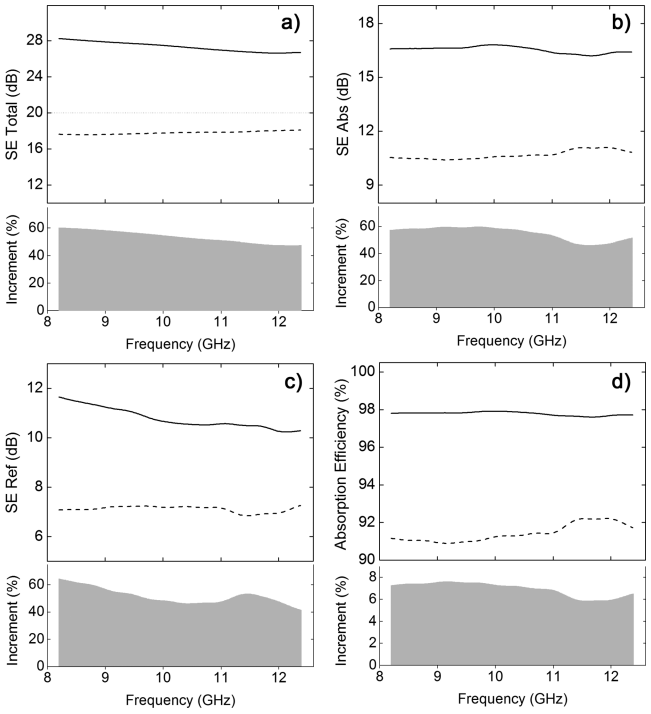

Figure 7. Total SE (a), SE absorption (b), SE reflection (c), and absorption efficiency (d) of neat CNF networks (dashed) and GN/CNF composite networks with 17.2 wt % GN (solid). Performance increments of the GN/CNF composite networks were calculated based on the performance in neat CNF networks.

performance in EMI shielding. Typically, Figure 7 shows the comparison of GN/CNF composite and neat CNF networks in the shielding performance, which suggests the contribution of interfacial modification by the CNF−GN−CNF heterojunctions. As exhibited in Figure 7a, GN/CNF composite networks demonstrate an effective total SE of 25−28 dB, reaching the commercial application level (>20 dB). These values are 50−60% higher than those found in the neat CNF networks (17−18 dB). Moreover, the corresponding SE absorption (up to 17 dB) and SE reflection (10−12 dB) observed in the GN/CNF composite networks were also higher than those observed in the neat CNF networks (Figure 7b and 7c). Interestingly, the increments in total SE, SE absorption, and SE reflection were almost around 40−60% (Figure 7), which is consistent with the increment observed in the electrical conductivity (Figure 4b). In addition, the mechanism for the effective SE in the GN/CNF composite networks should be mainly attributed to formation of much improved electrically conductive interconnections due to the presence of the CNF−GN−CNF heterojunctions. Furthermore, the absorption efficiency of GN/CNF composite networks reached ∼98% (Figure 7d), suggesting a highly sufficient contribution of electromagnetic absorption in the energy attenuation.

In Table 2, typical carbon-based composites and corresponding shielding performance were listed. Compared to the recent report,[1,2,9,10,12,14−16,28−36] the observed shielding performance (25−28 dB) in the GN/CNF composite networks is well comparable to that of the other typical carbon- and graphene-based materials (Table 2). It is noted that the density of the as-spun networks in this work was approximately estimated to be 0.08−0.1 g/cm^3, which indicates that the ratio of SE to density could be larger than 250 dB/(g/cm^3) in the GN/CNF composite networks. However, this ratio, so-called specific SE in some work,[9,12] is relatively insignificant in EMI shielding because shielding performance is substantially dependent on the propagating depth of electromagnetic waves and electrical conductivity of shielding materials.[5,22] Therefore, a comparison of specific SE based on previous work will not be considered even though this value in the GN/CNF composite networks here is considerably higher than the results achieved in the other related work. According to the relationship between electrical conductivity and materials thickness, increased electrical conductivity could effectively reduce the thickness of shielding materials since the propagating depth of the incident waves in the materials could be decreased.[5,16,22,25] In comparison with the strategy of mixing conductive fillers with polymeric matrices (Table 2), use of the entire conductive configuration in this work could effectively eliminate the poor contact and interfacial conductivity induced by the insulating polymers. Further enhancement could be achieved by optimizing the contact and bridging modes of the CNFs by employing CNF−GN−CNF heterojunctions. Compared to a recent work of directly dispersing GN into PEVA for fabricating composite films,[16] the all-carbon GN/CNF composite networks here present a better configuration, in which the

Table 2. Comparison of Typical Carbon-Based Materials and Corresponding Shielding Performance

fillers	matrices	thickness (mm)	electrical conductivity (S/m)	shielding performance (dB)	refs
CNT	polystyrene	1.0	>0.1	18−19	1
carbon fibers	polystyrene		>0.1	17−19	2
reduced graphene oxide	poly(methyl methacrylate)	2.4	3	13−19	9
functionalized graphene	polystyrene	2.5	1.25	25−29	10
reduced graphene oxide	poly(etherimide)	2.3	∼0.001	18−22	12
CVD-growth graphene	PDMS	1.0	200	22−25	14
reduced graphene oxide@Fe_3O_4	poly(etherimide)	2.5		14−18	15
reduced graphene oxide	paraffin wax	2.0	<0.1	18−29	34
fiber cloth-MWCNT-carbon areogel	PDMS		232	18−23	35
GN	PEVA	0.36	250	23−27	16
neat CNF networks		0.22−0.27	500	17−18	this work
CNF−GN networks		0.22−0.27	800	25−28	this work

thickness of the shielding materials could be further reduced (lower than 0.3 mm). Further opportunities for improvement include more sufficient carbonization or graphitization at much higher temperatures, whereby a significant increase of the electrical properties could be envisaged. For potential applications, use of CNF (as the flexible frame) and CNF−GN−CNF heterojunctions (as the interfacial modifier) has demonstrated a very promising all-carbon configuration for ultrathin shielding materials, which may meet the requirement in the lightweight flexible electronic devices. Additionally, the concept of establishing CNF−GN−CNF heterojunctions could be widely applied to various fields, where a unique structure or a specific application is required.

CONCLUSIONS

In summary, novel flexible all-carbon networks have been fabricated via the facile electrospinning processing. In the conductive networks with the presence of GN, CNF−GN−CNF heterojunctions have been observed to be the critical interfacial modifiers in the significant improvement of electrical conductivity, thus leading to the pronounced enhancement in the shielding effectiveness. The as-fabricated thin networks (material thickness < 0.3 mm) with lightweight (density < 0.1 g/cm^3) have also shown highly competitive EMI shielding performance to those carbon-based composites of much larger thickness (>1 mm). Therefore, the strategy for achieving flexible all-carbon networks based on the CNF−GN−CNF heterojunctions has demonstrated great potential in the scalable production of lightweight shielding materials for flexible portable electronic devices.

EXPERIMENTAL SECTION

GN. GN was prepared according to our previous work.[24,25] Briefly, the commercial graphite sample (0.5 g, grade 3805 from Asbury Carbons) was pretreated in alcohol aqueous solution for stirring and sonication. Dried pretreated samples were further dispersed in a mixture solution of nitric acid and sulfuric acid under sonication (48−72 h) for direct chemical exfoliation. The resulting samples were washed with deionized water and dried in a vacuum oven.

GN/CNF Composite Networks. GN/CNF composite networks were fabricated by the electrospinning technique. In a typical process, various amounts of GNs (20, 40, and 90 mg) were first dispersed in 4.5 g of DMF to obtain a homogeneous GN/DMF suspension using a sonicator and homogenizer. Subsequently, polyacrylonitrile (PAN, M_w = 150 000, Aldrich) (0.5 g) was added to the GN/DMF suspension, followed by vigorous stirring at 60 °C for 8 h. The above suspension was transferred into a 5 mL syringe equipped with a stainless steel nozzle (#8) and propelled at a flow rate of 0.010 mL/min (0.015 mL/min for samples with higher GN loadings). A high voltage of ∼15 kV was then applied between the nozzle tip and the collector with a distance of 150 mm. The electrospinning process was carried out at ambient temperature. Subsequently, the as-spun polymeric GN nonwoven mat was peeled off and then stabilized at 270 °C in air (1 h, heating rate 3 °C/min), followed by carbonization under nitrogen atmosphere at 1000 °C for 3 h (heating rate of 5 °C/min). The resulting GNs/CNF networks with different initial GN amounts were assigned in Table 1. For comparison, neat CNF networks as the reference sample were fabricated with the same procedure without adding GN.

Layered Structures. For accurate measurement of S parameters, layered structures have been fabricated to ensure the free-standing networks to be vertically positioned in the testing chamber.[16] Paraffin wax (Walgreen) and poly(ethylene-vinyl acetate) (PEVA) (DuPont Co.) were employed as the testing substrates and glue for fabricating the layered structures, respectively. Wax substrates with dimensions of 22.86 × 10.16 × 1 mm^3 (size of testing chamber) were prepared by cold press. PEVA was dissolved toluene, followed by evaporating most of the solvent to obtain viscous PEVA/toluene glue. All measured GN/CNF composite networks (including neat CNF networks) with a thickness of 220−270 μm were cut into a rectangular shape of 22.86 × 10.16 mm^2. In the fabrication of wax|GN/CNF composite networks|wax structures, GN/CNF composite networks were sandwiched into two pieces of wax substrates with PEVA/toluene glue. Similarly, the wax|neat CNF networks|wax structure was fabricated with the same approach. All layered structures were dried in ambient conditions to achieve testing samples.

Characterization. As-prepared GN/CNF composite networks were characterized by various techniques. X-ray diffraction (XRD) characterization was carried out on a Rigaku D/max-RB system. Raman spectra were investigated using a Jobin Yvon T64000 Raman spectrometer equipped with a Melles-Griot 35 mW He−Ne laser source for 633 nm excitation. Field emission scanning electron microscopy (FE-SEM) images were obtained on a ZEISS supra 55 system. Transmission electron microscopy (TEM) was performed on a TECHAI G220 Scanning-TEM system. For observing the cross-section view of the GN on the TEM, microtomed samples were prepared using a Reichert-Jung Ultracut E Microtome with a 30° angle diamond knife.[37,38] Electrical conductivity (σ) was determined using the classical four-probe method, with the electrical current (I) and voltage (V) relationship for the networks obtained by a multimeter (Keithley 2400, controlled by Lab Tracer 2.0 software, both from Keithley Instruments) and a multiheight probe (Jandel). With the relation of network thickness (d), the electrical conductivity for the networks was determined by the equation $\sigma = (\ln 2/\pi)(I/V)/d$. To ensure accuracy of the measurement for electrical conductivity, three different regions of both sides of the spun networks were selected for testing. The average electrical conductivity and corresponding errors (Figure 4a) of each sample were determined by the six measured values. The density of the spun networks was roughly estimated by the ratio of mass to volume. The weight and dimensions of a piece of spun networks were scaled three times to achieve the average values.

EMI Shielding. The S parameters (S_{11} and S_{21}) of the as-fabricated sandwich layered structures were measured on an Anritsu 37269D vector network analyzer (VNA) using the waveguide method in X band.[16,33] The power coefficients, reflection coefficient (R) and transmission coefficient (T), were calculated by the equations $R = |S_{11}|^2$ and $T = |S_{21}|^2$, respectively. Absorption coefficient (A) was obtained from the relation $A = 1 - R - T$.[16,33] Absorption efficiency (AE) was calculated by the relation AE = $A/(1 - R) \times 100\%$. EMI shielding effectiveness (SE_{tot}) refers to the logarithm of the ratio of the incident wave P_I to the transmitted wave P_T, which is determined by the equation $SE_{tot} = 10\log(P_I/P_T)$dB. The total experimental SE is the sum of the net shielding by reflection (SE_{ref}) and absorption (SE_{abs}), which can be given as $SE_{ref} = -10\log(1 - R)$dB and $SE_{abs} = -10\log(T/(1 - R))$dB, respectively.[16]

ASSOCIATED CONTENT

Supporting Information

EMI shielding performance of the GN/CNF composite networks with 9.4 wt % GN. This material is available free of charge via the Internet at http://pubs.acs.org.

AUTHOR INFORMATION

Corresponding Authors

*E-mail: fanlizhen@ustb.edu.cn.

*E-mail: caomaosheng@bit.edu.cn.

Notes

The authors declare no competing financial interest.

ACKNOWLEDGMENTS

Financial support from 973 Project (2013CB934001), NSF of China (Grant Nos. 51172024, 51372022, and 51302011), and China PSF (2012M520165) is gratefully acknowledged.

REFERENCES

(1) Yang, Y. L.; Gupta, M. C.; Dudley, K. L.; Lawrence, R. W. Novel Carbon Nanotube-Polystyrene Foam Composites for Electromagnetic Interference Shielding. *Nano Lett.* **2005**, *5*, 2131−2134.

(2) Yang, Y. L.; Gupta, M. C.; Dudley, K. L.; Lawrence, R. W. Conductive Carbon Nanofiber−Polymer Foam Structures. *Adv. Mater.* **2005**, *17*, 1999−2003.

(3) Li, N.; Huang, Y.; Du, F.; He, X. B.; Lin, X.; Gao, H. J.; Ma, Y. F.; Li, F. F.; Chen, Y. S.; Eklund, P. C. Electromagnetic Interference (EMI) Shielding of Single-Walled Carbon Nanotube Epoxy Composites. *Nano Lett.* **2006**, *6*, 1141−1145.

(4) Wang, J. C.; Xiang, C. S.; Liu, Q.; Pan, Y. B.; Guo, J. K. Ordered Mesoporous Carbon/Fused Silica Composites. *Adv. Funct. Mater.* **2008**, *18*, 2995−3002.

(5) Chung, D. D. L. Electromagnetic Interference Shielding Effectiveness of Carbon Materials. *Carbon* **2001**, *39*, 279−285.

(6) Chung, D. D. L. Carbon Materials For Structural Self-sensing, Electromagnetic Shielding and Thermal Interfacing. *Carbon* **2012**, *50*, 3342−3353.

(7) Wen, B.; Cao, M. S.; Hou, Z. L.; Song, W. L.; Zhang, L.; Lu, M. M.; Jin, H. B.; Fang, X. Y.; Wang, W. Z.; Yuan, J. Temperature Dependent Microwave Attenuation Behavior for Carbon-Nanotube/Silica Composites. *Carbon* **2013**, *65*, 124−139.

(8) Arjmand, M.; Apperley, T.; Okoniewski, M.; Sundararaj, U. Comparative Study of Electromagnetic Interference Shielding Properties of Injection Molded versus Compression Molded Multi-walled Carbon Nanotube/Polystyrene Composites. *Carbon* **2012**, *50*, 5126−5134.

(9) Zhang, H. B.; Yan, Q.; Zheng, W. G.; He, Z. X.; Yu, Z. Z. Tough Graphene-Polymer Microcellular Foams for Electromagnetic Interference Shielding. *ACS Appl. Mater. Interfaces* **2011**, *3*, 918−924.

(10) Yan, D. X.; Ren, P. G.; Pang, H.; Fu, Q.; Yang, M. B.; Li, Z. M. Efficient Electromagnetic Interference Shielding of Lightweight Graphene/Polystyrene Composite. *J. Mater. Chem.* **2012**, *22*, 18772−18774.

(11) Moglie, F.; Micheli, D.; Laurenzi, S.; Marchetti, M.; Primiani, V. M. Electromagnetic Shielding Performance of Carbon Foams. *Carbon* **2012**, *50*, 1972−1980.

(12) Ling, J. Q.; Zhai, W. T.; Feng, W. W.; Shen, B.; Zhang, J. F.; Zheng, W. G. Facile Preparation of Lightweight Microcellular Polyetherimide/Graphene Composite Foams for Electromagnetic Interference Shielding. *ACS Appl. Mater. Interfaces* **2013**, *5*, 2677−2684.

(13) Liu, Q. L.; Gu, J. J.; Zhang, W.; Miyamoto, Y.; Chen, Z. X.; Zhang, D. Biomorphic Porous Graphitic Carbon for Electromagnetic Interference Shielding. *J. Mater. Chem.* **2012**, *22*, 21183−21188.

(14) Chen, Z. P.; Xu, C.; Ma, C. Q.; Ren, W. C.; Cheng, H. M. Lightweight and Flexible Graphene Foam Composites for High-Performance Electromagnetic Interference Shielding. *Adv. Mater.* **2013**, *25*, 1296−1300.

(15) Shen, B.; Zhai, W.; Tao, M.; Ling, J.; Zheng, W. Lightweight, Multifunctional Polyetherimide/Graphene@Fe_3O_4 Composite Foams for Shielding of Electromagnetic Pollution. *ACS Appl. Mater. Interfaces* **2013**, *5*, 11383−11391.

(16) Song, W. L.; Cao, M. S.; Lu, M. M.; Bi, S.; Wang, C. Y.; Liu, J.; Yuan, J.; Fan, L. Z. Flexible Graphene/Polymer Composite Films in Sandwich Structures for Effective Electromagnetic Interference Shielding. *Carbon* **2014**, *66*, 67−76.

(17) Maiti, S.; Shrivastava, N. K.; Suin, S.; Khatua, B. B. Polystyrene MWCNT Graphite Nanoplate Nanocomposites: Efficient Electromagnetic Interference Shielding Material through Graphite Nanoplate−MWCNT−Graphite Nanoplate Networking. *ACS Appl. Mater. Interfaces* **2013**, *5*, 4712−4724.

(18) Singh, A. P.; Garg, P.; Alam, F.; Singh, K.; Mathur, R. B.; Tandon, R. P.; Chandra, A.; Dhawan, S. K. Phenolic Resin-based Composite Sheets Filled with Mixtures of Reduced Graphene Oxide, γ-Fe_2O_3 and Carbon Fibers for Excellent Electromagnetic Interference Shielding in the X-band. *Carbon* **2012**, *50*, 3868−3875.

(19) Gupta, T. K.; Singh, B. P.; Mathura, R. B.; Dhakate, S. R. Multi-walled Carbon Nanotube−Graphene−Polyaniline Multiphase Nanocomposite with Superior Electromagnetic Shielding Effectiveness. *Nanoscale* **2014**, *6*, 842−851.

(20) Yang, S. Y.; Lin, W. N.; Huang, Y. L.; Tien, H. W.; Wang, J. Y.; Ma, C. C. M.; Li, S. M.; Wang, Y. S. Synergetic Effects of Graphene Platelets and Carbon Nanotubes on the Mechanical and Thermal Properties of Epoxy Composites. *Carbon* **2011**, *49*, 793−803.

(21) Yu, A.; Ramesh, P.; Sun, X. B.; Bekyarova, E.; Itkis, M. E.; Haddon, R. C. Enhanced Thermal Conductivity in a Hybrid Graphite Nanoplatelet−Carbon Nanotube Filler for Epoxy Composites. *Adv. Mater.* **2008**, *20*, 4740−4744.

(22) Al-Saleh, M. H.; Sundararaj, U. Electromagnetic Interference Shielding Mechanisms of CNT/Polymer Composites. *Carbon* **2009**, *47*, 1738−1746.

(23) Liang, J. J.; Wang, Y.; Huang, Y.; Ma, Y. F.; Liu, Z. F.; Cai, J. M.; Zhang, C. D.; Gao, H. J.; Chen, Y. S. Electromagnetic Interference Shielding of Graphene/Epoxy Composites. *Carbon* **2009**, *47*, 922−925.

(24) Song, W. L.; Wang, W.; Veca, L. M.; Kong, C. Y.; Cao, M. S.; Wang, P.; Meziani, M. J.; Qian, H. J.; LeCroy, G. E.; Cao, L.; Sun, Y. P. Polymer/Carbon Nanocomposites for Enhanced Thermal Transport Properties-Carbon Nanotubes versus Graphene Sheets as Nanoscale Fillers. *J. Mater. Chem.* **2012**, *22*, 17133−17139.

(25) Song, W. L.; Fan, L. Z.; Cao, M. S.; Lu, M. M.; Wang, C. Y.; Wang, J.; Chen, T. T.; Li, Y.; Hou, Z. L.; Liu, J.; Sun, Y.-P. Facile Fabrication of Ultrathin Graphene Papers for Effective Electromagnetic Shielding. *J. Mater. Chem. C* **2014**, *2*, 5057−5064.

(26) Luo, C. J.; Stoyanov, S. D.; Stride, E.; Pelanb, E.; Edirisinghe, M. Electrospinning versus Fibre Production Methods: from Specifics to Technological Convergence. *Chem. Soc. Rev.* **2012**, *41*, 4708−4735.

(27) Inagaki, M.; Yang, Y.; Kang, F. Y. Carbon Nanofibers Prepared via Electrospinning. *Adv. Mater.* **2012**, *24*, 2547−2566.

(28) Liu, Z. F.; Bai, G.; Huang, Y.; Ma, Y. F.; Du, F.; Li, F. F.; Guo, T. Y.; Chen, Y. S. Reflection and Absorption Contributions to the Electromagnetic Interference Shielding of Single-walled Carbon Nanotube/Polyurethane Composites. *Carbon* **2007**, *45*, 821−827.

(29) Huang, Y.; Li, N.; Ma, Y. F.; Du, F.; Li, F. F.; He, X. B.; Lin, X.; Gao, H. J.; Chen, Y. S. The Influence of Single-walled Carbon Nanotube Structure on the Electromagnetic Interference Shielding Efficiency of Its Epoxy Composites. *Carbon* **2007**, *45*, 1614−1621.

(30) Arjmand, M.; Mahmoodi, M.; Gelves, G. A.; Park, S.; Sundararaj, U. Electrical and Electromagnetic Interference Shielding Properties of Flow-Induced Oriented Carbon Nanotubes in Polycarbonate. *Carbon* **2011**, *49*, 3430−3440.

(31) Wu, Z. F.; Wang, H.; Zheng, K.; Xue, M.; Cui, P.; Tian, X. Y. Incorporating Strong Polarity Minerals of Tourmaline with Carbon Nanotubes to Improve the Electrical and Electromagnetic Interference Shielding Properties. *J. Phys. Chem. C* **2012**, *116*, 12814−12818.

(32) Saini, P.; Choudhary, V.; Vijayan, N.; Kotnala, R. K. Improved Electromagnetic Interference Shielding Response of Poly(aniline)-Coated Fabrics Containing Dielectric and Magnetic Nanoparticles. *J. Phys. Chem. C* **2012**, *116*, 13403−13412.

(33) Cao, M. S.; Song, W. L.; Hou, Z. L.; Wen, B.; Yuan, J. The Effects of Temperature and Frequency on the Dielectric Properties, Electromagnetic Interference Shielding and Microwave-Absorption of Short Carbon Fiber/Silica Composites. *Carbon* **2010**, *48*, 788−796.

(34) Wen, B.; Wang, X. X.; Cao, W. Q.; Shi, H. L.; Lu, M. M.; Wang, G.; Jin, H. B.; Wang, W. Z.; Yuan, J.; Cao, M. S. Reduced Graphene Oxides: The Thinnest and Most Lightweight Material with High-efficient Microwave Attenuation Performances around Carbon World. *Nanoscale* **2014**, *6*, 5754−5761.

(35) Chen, M. T.; Zhang, L.; Duan, S. S.; Jing, S. L.; Jiang, H.; Luo, M. F.; Li, C. Z. Highly Conductive and Flexible Polymer Composites with Improved Mechanical and Electromagnetic Interference Shielding Performances. *Nanoscale* **2014**, *6*, 3796−3803.

(36) Kong, L.; Yin, X. W.; Yuan, X. Y.; Zhang, Y. J.; Liu, X. M.; Cheng, L. F.; Zhang, L. T. Electromagnetic Wave Absorption

Properties of Graphene Modified with Carbon Nanotube/Poly-(Dimethyl Siloxane) Composites. *Carbon* **2014**, *73*, 185−193.
(37) Song, W. L.; Cao, M. S.; Lu, M. M.; Liu, J.; Yuan, J.; Fan, L. Z. Improved Dielectric Properties and Highly Efficient and Broadened Bandwidth Electromagnetic Attenuation of Thickness-Decreased Carbon Nanosheet/Wax Composites. *J. Mater. Chem. C* **2013**, *1*, 1846−1854.
(38) Song, W. L.; Wang, P.; Cao, L.; Anderson, A.; Meziani, M. J.; Farr, A. J.; Sun, Y.-P. Polymer/Boron Nitride Nanocomposite Materials for Superior Thermal Transport Performance. *Angew. Chem., Int. Ed.* **2012**, *51*, 6498−6501.